AD-A191 006 EFFICIENT HIGH RESOLUTION COMPUTATIONS OF PROJECTILE AND MISSILE FLOW FIELDS(U) PEDA CORP PALO ALTO CA C K LOMBARD ET AL. DEC 87 ARO-21247.6-EG-S 1/1

UNCLASSIFIED DAAG29-84-C-0002 F/G 20/4 NL

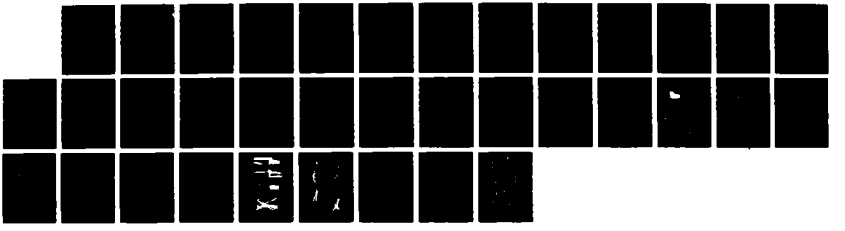

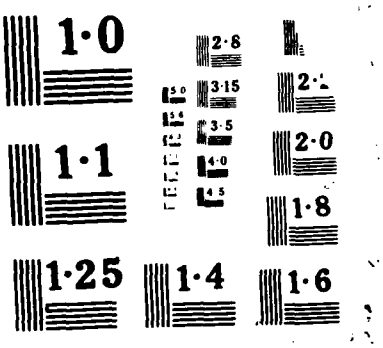
1·0
1·1
1·25
1·4
1·6
1·8
2·0
2·2
2·5
2·8
3·15
3·5
4·0
4·5

AD-A191 086

REPORT DOCUMENTATION PAGE

1a. RESTRICTIVE MARKINGS: Unclassified	1b. RESTRICTIVE MARKINGS
2a. SECURITY CLASSIFICATION AUTHORITY	3. DISTRIBUTION/AVAILABILITY OF REPORT: Approved for public release; distribution unlimited.
2b. DECLASSIFICATION/DOWNGRADING SCHEDULE	
4. PERFORMING ORGANIZATION REPORT NUMBER(S)	5. MONITORING ORGANIZATION REPORT NUMBER(S): ARO 21247.6-EG-S
6a. NAME OF PERFORMING ORGANIZATION: PEDA Corporation; 6b. OFFICE SYMBOL (If applicable)	7a. NAME OF MONITORING ORGANIZATION: U. S. Army Research Office
6c. ADDRESS (City, State, and ZIP Code): 4151 Middlefield Road, Suite 7, Palo Alto, CA 94303	7b. ADDRESS (City, State, and ZIP Code): P. O. Box 12211, Research Triangle Park, NC 27709-2211
8a. NAME OF FUNDING/SPONSORING ORGANIZATION: U. S. Army Research Office; 8b. OFFICE SYMBOL (If applicable)	9. PROCUREMENT INSTRUMENT IDENTIFICATION NUMBER: DAAG29-84-C-0002
8c. ADDRESS (City, State, and ZIP Code): P. O. Box 12211, Research Triangle Park, NC 27709-2211	10. SOURCE OF FUNDING NUMBERS: PROGRAM ELEMENT NO. / PROJECT NO. / TASK NO. / WORK UNIT ACCESSION NO.

11. TITLE (Include Security Classification)
EFFICIENT, HIGH RESOLUTION COMPUTATIONS OF PROJECTILE AND MISSILE FLOW FIELDS

12. PERSONAL AUTHOR(S)
C.K. Lombard, Jorge Bardina, R.C.-C. Luh and Ethiraj Venkatapathy

13a. TYPE OF REPORT	13b. TIME COVERED	14. DATE OF REPORT (Year, Month, Day)	15. PAGE COUNT
FINAL	FROM 84 3 15 TO 87 9 14	87 12 22	31

16. SUPPLEMENTARY NOTATION
The view, opinions and/or findings contained in this report are those of the author(s) and should not be construed as an official Department of the Army position, policy, or decision, unless so designated by other documentation.

17 COSATI CODES		
FIELD	GROUP	SUB-GROUP

18. SUBJECT TERMS (Continue on reverse if necessary and identify by block number)
Algebraic Grid Generation, Navier-Stokes, Upwind Methods, Projectile Flow, Missile Flow, Base Flow, Adaptive Grid, Composite Grid, Overset Grid

19. ABSTRACT (Continue on reverse if necessary and identify by block number)

A new family of computational tools is explored in the context of generic problems of interest to Army Research and Development missions. The problems are the SOCBT projectile flow and the MICOM model tactical base flow. Both problems, for which experimental data is available for comparison, have also been extensively computed by other groups with other methods, principally the central difference method of Beam and Warming.

Here the techniques we employ and to some extent refine are composite and overset patched mesh systems generated with a new multistep, graphics interactive algebraic procedure FASTWO and the CSCM-S symmetric Gauss-Seidel relaxation procedure. The grid generation technique permits comparatively simple direct user control of mesh spacing and quality.

The CSCM-S algorithm is an alternating direction space marching method of lines in 2-D and planes

20. DISTRIBUTION/AVAILABILITY OF ABSTRACT	21. ABSTRACT SECURITY CLASSIFICATION
☐ UNCLASSIFIED/UNLIMITED ☐ SAME AS RPT. ☐ DTIC USERS	Unclassified
22a. NAME OF RESPONSIBLE INDIVIDUAL	22b. TELEPHONE (Include Area Code) / 22c. OFFICE SYMBOL

19. ABSTRACT continued

in 3-D. The method is economical both in storage and data handling and, also, is rapidly convergent as the result of improved propagation of nonlinear advection, boundary to boundary. In the SOCBT problem the method exhibited convergence in order 100 global iterations and showed improved accuracy *vis a vis* central difference methods in capturing features of the flow such as shocks and expansions. The method is stable in both elliptic regions and zones of streamwise separated flow including base flow.

In the MICOM base flow problem effects of mesh topology and resolution were elucidated. It was found that wraparound grid topology communicating the boundary layer at base corners is helpful. The use of multiple independent patched meshes achieves better balanced resolution and use of mesh resources. Finally, flow structure adaptive grid redistribution can markedly impact accuracy of flow structure capture and fundamentally alter the character of coupled vortex interactions in base flow. Within the context of these experiments, all computed with the same classical algebraic mixing length eddy viscosity wake model that was not tuned in any respect, the evidence is that grid quality is of paramount significance in getting the flow right.

ARO 21247.6-EG-S

EFFICIENT, HIGH RESOLUTION COMPUTATIONS OF PROJECTILE AND MISSILE FLOW FIELDS

Final Report

C.K. Lombard, Jorge Bardina, R. C.-C. Luh and Ethiraj Venkatapathy

December 1987

U.S. Army Research Office

DAAG29-84-C-0002

PEDA Corporation
4151 Middlefield Road, Suite 7
Palo Alto, California 94303
(415) 493-5123

Table of Contents

Figure Titles

1. Introduction

Based on the Beam-Warming central difference algorithm[1,2] of the late seventies and with the increasing power of scientific computers, the early eighties saw a substantial computational effort[3-16] at analyzing projectile and missile flowfields. The early work[3-9] focused particular attention on the important Secant-Ogive-Cylinder-Boattail (SOCBT) projectile configuration for which a substantial body[5,6,7,17] of experimental results had been obtained. The results of an assessment[18] made shortly before the present work was initiated may be summarized as follows. At zero angle of attack or away from the immediate transonic zone $.9 < M < 1.1$, the subsonic and supersonic techniques using the thin layer Navier-Stokes approximation[19] in respective time[1] and space marching[2] implementations of Beam and Warming factored implicit numerical methods had been found effective in flow field predictions and the derived aerodynamic coefficients. In the immediate transonic regime where aerodynamic coefficients are a highly nonlinear and rapidly varying function of Mach number, performance had not been as satisfactory. In the later regime, the variation of coefficients is largely governed[5,7] by the sensitive movements of shocks, aftward with increasing Mach number; and computational accuracy and numerical stability become of major importance. Intimately related to the shocks are precursor expansions which are equally difficult and important to treat accurately. A final computational detail needing improvement was the ability to accurately compute flow in the vicinity of contact discontinuities which appear in streamwise and cross flow separations, for example.

Another emerging computation area was base flow analysis which became an important research topic for both[18] the impacts on drag and pitching moment. Base flow computations were performed for projectiles[7] and, with more emphasis[10-16], on a wind tunnel model tactical missile with centered propulsive jet. The latter computations provided universally unsatisfactory predictions of base pressure, a deficiency largely ascribed at the time to inadequate turbulence modeling.

In the same time frame of these early computations, PEDA Corporation was carrying out research and development to provide advanced computational tools for viscous flow analyses in complicated geometries. The theme of the research was accurate, efficient flux difference split implicit upwind schemes[20-25] that did not require *ad hoc* smoothing operators and efficient high quality algebraic grid generation[26] on domain boundary fitting patch mesh systems.

The flux difference split upwind implicit schemes with coupled well posed characteristic boundary point approximations were known to have superior natural stability properties while providing sharper capture of flow structures such as shocks, expansions and contacts. A newly discovered symmetric Gauss-Seidel relaxation scheme CSCM-S[24,25] for the CSCM upwind method[20-23] had been found to be both more efficient in data storage and handling but, also, to be substantially more rapidly convergent to steady state.

The complementary development, algebraic grid generation in patched mesh systems, had the fundamental capability to provide direct control[26,27] of mesh topology, spacing and quality without the necessity and numerical complexity of solving sets of partial differential equations, as was being practiced[28] in some prominent lines of development.

Problem Statement

The intent of the presently reported effort was to implement, test and demonstrate the applicability and effectiveness of the evolving new computational methodology in the analysis of problems of interest to US Army research and development. Based on both theory and numerical experience, the belief was that the new methods had the potential to improve accuracy, efficiency and productivity in aerodynamic design analysis.

In the next section we will summarize the substantial effort that has been made in adapting tools and exploring the numerical solution of two generic transonic aerodynamics problems – SOCBT and MICOM missile base flow – of direct Army interest and for which good experimental and computational background exist.

2. Research Accomplished

Over the nominally three year program we have explored the 2-D axisymmetric problems of the SOCBT forebody and base flow and MICOM missile base flow. That work has resulted in six meeting papers[29–34] reporting different advances and understandings obtained in the course of attacking these problems. We have also studied 3-D flows about the SOCBT at angle of attack. In the latter part of the program we requested and obtained a six month no cost extension permitting us under other support to further advance our 3-D computational tools – algebraic grid generation and the CSCM-S algorithm. The latter improved program[35] has been employed in the 3-D angle of attack computations for the SOCBT that we report on here and elsewhere[36].

Algebraic Grid Generation

The concept of patched meshing in which complex domains are broken up into many geometrically regular and topologically rectangular subdomains leads naturally to the use of efficient algebraic techniques for the construction of the individual mesh patches. To obtain the desired smoothness properties over the global mesh in the vicinity of patch boundaries, comparatively early in our methods research, a technique that permits specification of point distribution and gradient on all boundaries had been devised. The technique – termed generalized transfinite interpolation[26] – can be seen to embed use of a parameterized general cubic polynomial for the coordinate curves. Regularity of the mesh is obtained by employing continuous distributions of the parameters of the curves within judiciously chosen bounds based on analysis. Stretching functions such as that of Vinokur[37] are used

to distribute points and blending functions are used to distribute parameters of the curves between lateral boundaries.

A novel feature of the technique was the introduction of the corner singularity from analysis to govern distribution of points and parameters in the vicinity of boundary slope singularities. At such points, the method thus obtains the desired properties of mesh smoothness to the interior.

However, in attempting to apply the generalized transfinite interpolation technique in a variety of 2-D problems, it became evident the method was too sensitive to parameter selection among too many options, was confusing and ultimately required too much artistry to meet the objectives of simplicity and user friendliness set for the products of the research. Further, the lack of an analytical solution to corner problems blocked the straightforward extention of the technique to 3-D.

With some reflection it became evident to us early in the present program that the difficulty lay in trying to accomplish too much in a single step process. Rather, borrowing the tools of the algebraic technique and redefining the process in a sequence of simple steps with interactive computer graphics, we could define a straightforward procedure to meet the desired ends.

The fundamental approach that we employ and which was initially implemented under other support is in the realm of two boundary methods, in that one pair of opposite sides of a patch is regarded as prescribed and often includes a portion of a physical boundary. The other pair of sides is formed of the left and right limiting members of the family of generalized cubic coordinate curves joining the initially given two boundaries. In either 2-D or 3-D the general cubic coordinate curve has the simple form

$$\underline{r} = \underline{r_1} + (\underline{r_2} - \underline{r_1})f(u) + \underline{\sigma_1}g(u) + \underline{\sigma_2}h(u) \qquad (1)$$

where

$$f(u) = u^2(3 - 2u)$$
$$g(u) = u(1 - u)^2$$
$$h(u) = u^2(u - 1)$$

Equation (1) is a hermite interpolation of value ($\underline{r}$) and gradient ($\underline{\sigma}$) on the two boundaries and is parameterized in terms of u which varies from zero to unity. The scalings of $\underline{\sigma_1}$ and $\underline{\sigma_2}$ influence the shape (curvature) of the curve between any pair of end points. The specification of a discrete set of u values using a generalized distribution function such as that of reference 37 defines the nodal intersections with the other family of coordinate curves.

In our implementation, the left and right limiting (lateral bounding) coordinate curves are developed interactively on a graphics terminal or workstation to have the desired configurations. The parameters of these lateral bounding curves are then blended with polynomial weighting functions to describe the general cubic coordinate curve over the intervening, also discretized, interval.

The lateral patch boundaries are essentially control devices that specify shape and distribution to surrounding regions. As such they are placed where needed – at breaks in body surface geometry and as terminators or transition guides from regions of strong shape variation to regions of very regular mesh. In fact the mesh generation problem, particularly for geometries with any substantial complexity, is a problem of multiple length scales. The purpose of multiple patching is to isolate regions of comparable scales and on which subdomains the solution is comparatively regular and can be conveniently fit by simple functions.

Once a primary grid is generated by the technique described above it can be interactively improved by modifying parameter blending and point distribution including point redistribution along the alternate family of coordinate lines implicitly defined by the nodes on the cubic coordinate curves. The latter operation is in the spirit, if not the detailed implementation, of a two step generalized transfinite interpolation.

Another secondary operation that we employ is the modification of coordinate lines in the vicinity of a boundary to smoothly enforce local normality. The latter operation like all the procedures has been programmed as a convenient tool requiring minimal input to apply at a boundary. Finally, a parameterized tension spline[27] that provides an analytical description of a curve amongst discrete data is a tool that has proved useful in the latter operation, in effecting redistribution of points along coordinate curves of either family and for fitting numerically specified boundary data.

Under ARO support we have explored the application of the simplified multistep technique to the projectile and missile problems we have attacked computationally. In the course of the work and particularly over the first two years, we have progressively identified ways of improving the organization of the tools to provide better user control of mesh quality and enhanced productivity. The tools and organization of patched grid generation in five algebraic steps are described in references 33 and 34. The five step procedure (FASTWO in 2-D) that has evolved is

Step 1. Boundary definition for the global computational domain
Step 2. Wireframe block (patch) decomposition of the computational domain
Step 3. Trial grid generation
Step 4. Grid distribution adjustments
Step 5. Grid normalization at boundaries.

Over the past three years, the work has been very effectively employed in other Army R & D programs – notably grids for coupled external/cavity flow simulations in the transonic (AOA aircraft)[39] and hypersonic (HEDI missile)[40,41] speed regimes for USA-SDC. The work is presently finding application with USA-BRL in an analysis for sabot separation.

Many examples of grids generated with the technique are given in the references to our work. Here, for illustration, we show in Figures 1a, 1b, 1c and 1d the

wire frame domain decomposition for the SOCBT problem and three views of the resulting grid.

SOCBT Flows with the CSCM-S Algorithm

The technique that we have applied under the contract is a new single level operationally explicit but effectively implicit algorithm[24] for gasdynamics. The algorithm is particularly appropriate for multiple patch mesh systems because through the interior boundary treatment[42] each solution sweep operation on any patch can be decoupled from any other. Thus the method is not only very storage efficient and simple to program including the coupling at patch boundaries; but, also, can make excellent use of parallel computing in several straightforward ways.

Previously the Beam-Warming factored implicit algorithm[1] with the Baldwin-Lomax thin layer viscous approximation[19] has provided the basis for two similar space marching (PNS) procedures[2,43] for the compressible Navier-Stokes equations. These PNS methods which are highly efficient – requiring half the data storage and a small fraction of the computer time of two level time dependent methods – have proven effective for flows[10] with favorable streamwise pressure gradient or with relatively small adverse pressure gradients. However, in the presence of a strong adverse pressure gradient such as occurs in a wing or fin root regions the contemporary PNS methods suffer numerical stability problems and may infer streamwise separation even where separation doesn't occur[44]. In such unseparated (perhaps weakly separated) regions, numerical stability has been maintained at the price of employing large amounts of artificial viscosity with a resulting loss in predictive accuracy and knowledge of the actual state of the flow. Where strong streamwise separation occurs the methods are unstable and cannot proceed. Streamwise separation becomes a likely occurrence in fin roots and on deflected control surfaces and base regions. Thus a more general technique is needed that is inherently stable for all types of upstream influence. At a minimum the mixed elliptic-hyperbolic problem requires global iteration, preferably with type dependent differencing. More background on this problem area is given in reference 24.

Universal Single Level Scheme CSCM-S

The CSCM flux difference eigenvector split upwind implicit method[20–23] for the inviscid terms of the compressible Navier-Stokes equations provides the natural basis for an unconditionally stable space marching technique through regions of subsonic and streamwise separated flow. In such regions the split method can be likened to stable marching of each scalar characteristic wave system in the direction of its associated eigenvalue (simple wave velocity). In supersonic flow, where all eigenvalues have the same sign, the method automatically becomes equivalent to the referenced PNS techniques based on the Beam-Warming factored implicit method with the Baldwin-Lomax thin layer viscous approximation.

Compared to contemporary central difference methods, the CSCM characteristics based upwind difference approximation with its inherent numerical stability

leads to greatly reduced oscillation and greater accuracy in the presence of captured discontinuities such as shocks, contacts and physical or computational boundaries. The method has well validated heat transfer capability[45-47]. The correct mathematical domains of dependence that correspond with physical directions of wave propagation are coupled with well posed characteristic boundary approximations[23] naturally consistent with the interior point scheme. The result is a faster sorting out of transient disturbances and substantially more rapid convergence to the steady state. The splitting and the associated time dependent implicit method have been described in detail in references (20) and (23) respectively for quasi 1-D and 2-D planar or axisymmetric flow.

In the following, we will sketch the differences between the time dependent method and the space marching technique which we have designated CSCM-S. The discussion will begin with the quasi 1-D inviscid formulation, then give additional details entering into multidimensional inviscid and thin layer viscous procedures and present some 2-D axisymmetric solutions for the SOCBT. Lastly we sketch a 3-D implicit method of planes algorithm and give some results for the SOCBT at angle of attack.

Quasi 1-D Formulation

The general jth interior point difference equations for the time dependent CSCM upwind implicit method for the inviscid advection terms is

$$(I + \tilde{A}^{+}\nabla + \tilde{A}^{-}\Delta)\delta q_j = -\tilde{A}^{+}\Delta q)^{n}_{j-1} - \tilde{A}^{-}\Delta q)^{n}_{j} \tag{2}$$

where ∇ and Δ are backward and forward spatial difference operators. Here q is the conservative dependent variable vector and F is the associated flux vector. In the notation the interval averaged matrices between node points j and $j+1$ are indexed j. For simplicity, the right hand side of equation (2) is written for the first order method. Higher order methods in space are given with results in references 20, 23 and 38. In equation (2) the CSCM flux difference splitting is

$$(\tilde{A}^{+} + \tilde{A}^{-})\Delta q \equiv \Delta F^{+} + \Delta F^{-} = \Delta F \tag{3a}$$

with

$$\tilde{A}^{\pm} = (\overline{MT}I^{\pm}\overline{T}^{-1}\overline{M}^{-1})\tilde{A} \equiv \hat{A}^{\pm}\tilde{A} \tag{3b}$$

and

$$I^{\pm} = \frac{1}{2}(I \pm \mathrm{sgn}(\overline{\Lambda})) \tag{3c}$$

exhibiting the similarity transformation that diagonalizes the constructed[20,23] flux difference Jacobian $\tilde{A}$. Here $\overline{\Lambda}$ is a diagonal matrix of the interval averaged eigenvalues that through the truth function diagonal matrices $I^{\pm}$ make the decisions about directions of characteristic wave propagation and whether or not to send

signal to the solution point. Thus in equation (2) the piece of the flux difference splitting $\widetilde{A}^{+}\Delta q)_{j-1}$ represents the convection of characteristic wave contributions in the positive coordinate direction from grid point $j-1$ to solution point j and $\widetilde{A}^{-}$, in the negative direction from $j+1$ to j. As the result of incorporating multiplicatively the (local) time step (for pseudo time relaxation) and the spatial (divided) differences in the matrices, the numerical eigenvalues are Courant numbers for the characteristic waves whose speeds are u, $u+c$ and $u-c$, with c the sound speed.

Central to its accurate shock capturing capability, the CSCM conservative flux difference splitting has the Roe[48] "property U" embodied in equation 3a.

With $\delta q = q^{n+1} - q^{n}$, equation (2) defines a two level linearized coupled block matrix implicit scheme that can be solved by a block tridiagonal procedure. In reference (23) a new (DDADI) approximately factored alternating sweep bidiagonal solution procedure for equation (2) is presented that is shown to be very robust and is operationally explicit, i.e. requires only a decoupled sequence of local block matrix inversions rather than the solution of the coupled set. For the forward sweep the bidiagonal solution procedure can be written

$$(I + \widetilde{A}^{+} - \widetilde{A}^{-})\delta q^{*}{}_{j} = RHS + \widetilde{A}^{+}\delta q^{*}{}_{j-1} \tag{4}$$

For the linear problem, i.e. constant coefficient case of stability analysis, equation (4) is equivalent to the single level space marching procedure

$$(I + \widetilde{A}^{+} - \widetilde{A}^{-})\delta q^{*}{}_{j} = \widetilde{A}^{+}q^{*}{}_{j-1} - \widetilde{A}^{+}q^{n}_{j} - \widetilde{A}^{-}\Delta q)^{n}_{j} \tag{5}$$

Nonlinearity enters in the single level space marching form (5) in that at each step of the forward sweep the matrices $\widetilde{A}^{+}$ are averaged between $q^{*}{}_{j-1}$ and q^{n}_{j} rather than homogeneously at the old iteration level n. Similarly, a companion backward space marching sweep that is symmetric to equation (5) and that is intimately related to the backward sweep of the alternating bidiagonal algorithm of reference (23) is

$$(I + \widetilde{A}^{+} - \widetilde{A}^{-})\delta q_{j} = -\widetilde{A}^{+}\Delta q^{*})_{j-1} + \widetilde{A}^{-}q^{*}_{j} - \widetilde{A}^{-}q^{n+1}_{j+1} \tag{6}$$

The method given by equations (5) and (6) is von Neumann unconditionally stable for the scalar wave equation. The analysis shows the significance of DDADI approximate factorization in rendering both the forward and backward sweeps separately stable regardless of eigenvalue sign. Consequently as the local Courant number becomes very large, the robust method becomes a very effective (symmetric Gauss-Seidel) relaxation scheme for the steady equations, a fact which substantially contributes to the very fast performance that will be demonstrated.

At a right computational boundary on the forward sweep we solve the characteristic boundary point approximation[21,23]

$$(\widetilde{\widetilde{A}}^{+} + \widetilde{A}^{+})\delta q^{*}_{N} = \widetilde{A}^{+}q^{*}_{N-1} - \widetilde{A}^{+}q^{n}_{N} \tag{7}$$

$q_N^{n+1} = q_N^*$ and at a left, on the backward sweep

$$(\widetilde{\widetilde{A}}^- - \widetilde{A}^-)\delta q_1 = \widetilde{A}^- q_1^n - \widetilde{A}^- q_2^{n+1} \tag{8}$$

Following the solution of equations (7) and (8) the conservative state vector is iteratively corrected[21,23] to maintain the accuracy of prescribed boundary conditions while not disrupting the representation of the computed characteristic variables running to the boundary from the interior. Analysis of a model system with upwind differenced scalar equations and coupled boundary conditions was related to the linearized bidiagonal scheme[23] by Oliger and Lombard[49]; the analysis also strongly supports the numerically confirmed robust stability of the present nonlinear method for gasdynamics. A useful result of reference 49 that simplifies the procedure of reference 23 is that on the forward sweep there is no need for a predictor step at the left boundary $J = 1$; thus, the solution sweep begins at $J = 2$. Similarly, the backward sweep begins at $J = N - 1$.

With the updating at each step, where in equation (6) $\delta q_j = q_j^{n+1} - q_j^*$, it is clear that the symmetric pair of equations (5) and (6) serve to advance the solution two pseudo time (iteration) levels; whereas, the linear alternating bidiagonal sweep algorithm of reference (23) advances the solution only one level. To maintain conservation to a very high degree, in single sweep marching in supersonic zones we iterate (at least) once locally at each space marching step. The local iteration serves to make the eigenvectors in the coefficient matrices consistent with the advanced state and thus provides improved accuracy for the nonlinear system. It appears effective to do this inner iteration everywhere, i.e. in both subsonic and supersonic regions, as the number of global iteration steps to convergence with two inner iterations has been found reduced by a factor of three to four. Since the computational work per two steps is about the same for the single level and two level schemes, and beyond the fact that one saves a level of storage in the space marching algorithm, the question arises: Can one get solutions in less computational work through faster convergence with the nonlinear space marching algorithm?

With the globally iterative nonlinear space marching formulation, early experience[24] in two quasi 1-D nozzle problems with mixed supersonic-subsonic zones is that solutions are obtained in roughly an order of magnitude fewer iteration steps than had been required with the previously fast pseudo time dependent technique and block tridiagonal solving.

Two Dimensional Formulation

For two dimensional flow, assuming a marching coordinate ξ, inviscid terms

$$B^+ \nabla_\eta + B^- \Delta_\eta \tag{9a}$$

and

$$-B^+ \Delta_\eta q)_{k-1} - B^- \Delta_\eta q)_k \tag{9b}$$

are added to the left and right hand sides respectively of both the forward and backward sweep equations (5) and (6). For viscous flow, second centrally differenced, thin layer viscous terms are also added in the η direction as is conventionally practiced, e.g. Steger[50]. With the terms for the η cross marching coordinate direction, the technique now becomes an implicit method of lines. Along each η coordinate line, one can solve the equations coupled with a block tridiagonal procedure. Alternatively, a further DDADI bidiagonal approximate factorization can be employed in the η direction and solved either linearly as in reference (23) or nonlinearly as here in the ξ direction. As shown in the quasi 2-D numerical experiments of reference (23), DDADI bidiagonal approximate factorization is stable for viscous as well as inviscid terms. Finally in reference (23) there is a relevant discussion of the reduced approximate factorization error that attends using DDADI in one or more space directions.

SOCBT Axisymmetric Flow

In the course of the computational analyses[29] we simulated viscous transonic flows at Mach numbers .9, .94, .96, .98 and 1.1. Various approximations[29] of base/wake treatment with respect to the free flying projectile and wind tunnel sting mount were undertaken. These can be seen in the Mach contour plots of Figures 2a and 2b. In supersonic flow, for the case of the continued boattail sans base flow/wake region, Figure 2a, one loses the detail of a corner expansion followed by a lip shock that occurs with a backward step, Figure 2b. For comparison, C_p plots for the two cases are shown in Figures 3a and 3b. The low pressure of the base expansion is lost with the extended sting approximation.

For the high subsonic regime, Figures 4a, 4b, 4c and 4d, the base pressures can be seen to be slightly underpredicted for even the sting mounted case, Figure 4c, *vis a vis* the free flight geometry, Figure 4d. In both supersonic and subsonic flows, Figures 3a and 4b, the upwind differencing scheme produced qualitatively sharper responses to flow structures and in better agreement with experiment than the earlier computations with central differencing, with the attendant smoothing.

More details concerning the experiment and computational results can be found in references 17, 5 and 29.

Three Dimensional Method of Planes Algorithm

In reference 24 we presented a symbolic algebra for DDADI approximate factorization and derived single level relaxation schemes. The algebra is based on the implicit difference stencil of the implicit method. Here we use the approach to derive the symmetric Gauss-Seidel implicit method of planes relaxation algorithm employed in the present work.

The unfactored three dimensional linearized implicit method can be represented

by the symbolic matrix expression

$$\begin{array}{ccccc} & & B^- & & \\ & & & C^- & \\ -A^+ & & D & & A^- \\ & -C^+ & & & \\ & & -B^+ & & \end{array}$$

On the block diagonal the matrix $D = I + A^+ - A^- + B^+ - B^- + C^+ - C^-$. A once DDADI approximate factorization in the η coordinate direction leads to the expression

$$\begin{array}{ccccc} & B^- & & & \\ & & C^- & & \\ -A^+ & D & & & \\ -C^+ & & & & \\ & -B^+ & & & \end{array} \quad \bullet \quad D^{-1} \quad \bullet \quad \begin{array}{ccc} B^- & & \\ & C^- & \\ D & & A^- \\ -C^+ & & \\ -B^+ & & \end{array}$$

By analogy with the derivation of the single level scheme for quasi 1-D flow from DDADI bidiagonal approximate factorization, we identify the above expression with the alternate space marching implicit method of planes algorithm

Forward Sweep

$$\begin{bmatrix} & B^- & \\ -C^+ & D & C^- \\ & -B^+ & \end{bmatrix} \delta q_j^n = RHS[\, q_{j-1}^{n+1} \,,\, q_j^n \,]$$

Backward Sweep

$$\begin{bmatrix} & B^- & \\ -C^+ & D & C^- \\ & -B^+ & \end{bmatrix} \delta q_j^{n+1} = RHS[\, q_j^{n+1} \,,\, q_{j+1}^{n+2} \,]$$

In the planes the coupled block matrix problem can be further simplified by the approximate factorization

$$[\, -C^+ \,,\, D \,,\, C^- \,]\, D^{-1}\, [\, -B^+ \;\; D \;\; B^- \,] \delta q = RHS \tag{10a}$$

which leads directly to the block tridiagonal solution sequence

$$[\, -C^+ \;\; D \;\; C^- \,] \delta q^* = RHS \tag{10b}$$

$$[\, -B^+ \;\; D \;\; B^- \,] \delta q = D \delta q^* \tag{10c}$$

SOCBT Flow at Angle of Attack

Here the 3-D CSCM-S method has been applied to predict the aerodynamic flow field of a projectile configuration flying at Mach number 0.96, 0.98, and 1.1 at 4° angle of attack, and Mach number 0.95 at 2° angle of attack. The predictions show agreement in the quantitative and qualitative nature of the flow field, including the recirculatory base flow, and the comparisons with experimental data and other numerical results. Pressure measurements for this projectile supported by a base-mounted sting were made by Kayser and Whiton[17]. The present calculations were done with a grid which contained 128 longitudinal, 56 normal, and 31 circumferential points. Due to the symmetry plane imposed by the angle of attack of the mean flow and the axisymmetric geometry of the projectile, only half of the domain was simulated. Figure 5 shows the 99 by 31 grid configuration on the projectile surface. The 3-D grid was generated by rotating the 2-D grid of Figures 1 about the projectile axis of symmetry.

For a free stream Mach number of 0.96 and 4° angle of attack, Figure 6a shows the computed distribution of the surface pressure coefficient in the windward and leeward planes together with the square and circle symbols showing the experimental measurements. The expansions and recompressions near the ogive-cylinder and cylinder-boattail junctions are well captured by the simulations. The agreement with the experimental data is better on the ogive and cylinder surfaces than on the boattail surface.

Figure 6b shows the comparison obtained by Sahu[51] for this projectile configuration. As in the case of the 2-D simulations, the upwind method is in generally better qualitative agreement with experiment in following flow structure details than the central difference methods. A Mach contour plot for the solution of Figure 6a is shown in Figure 7.

Figure 8a shows the CSCM-S computed distribution of the surface pressure coefficient in the leeward plane with a free stream Mach number 0.95 and 2° angle of attack. Figure 8b shows three different predictions obtained by Nietubicz et al[52] with different numerical methods for a projectile with a similar configuration and a 7.5° boattail angle. The CSCM predictions agree better with the VSYM3D predictions obtained with the finer grid.

Additional computational results for 3-D angle of attack solutions will be presented in reference 36.

The present initial results show the predictive computational aerodynamic capabilities of the 3-D CSCM method for projectiles at transonic velocities. As in cases run at higher Mach numbers, the 3-D code predictions are in quite good agreement with results from the well validated 2-D CSCM codes. This efficient numerical method requires about one hour of Cray-XMP computer time for each three-dimensional simulation, while the present results have been verified by using an additional hour per calculation. The method provides a promising computational

capability to simulate the full flow field around projectiles, including the separated base flow.

MICOM Missile Base Flow

Various aspects of computational technique were explored in the context of the MICOM tactical missile model base flow experiment[15]. The axisymmetric problem was tested in a Mach 1.4 freestream. The model featured a broad flat base five times the exit diameter of an axis centered cold propulsive jet emitted from the base. The jet exit Mach number was 2.7 and the flow was underexpanded with normal pressure ratio of 2.15 relative to freestream.

We were particularly interested to study the effects of mesh topology and resolution on the prediction of base pressure, which was available from the experiment and had not previously been successfully simulated. All computational experiments were performed with the same classical mixing length wake model[30].

Figures 9a, 9b, 9c, and 9d show four meshes that were studied – respectively termed double wraparound, Cartesian step and independent multiple patched, the latter without and with computed flow structure adaptive grid redistribution[53]. Figures 10a, 10b, 10c, and 10d show the corresponding Mach contour plots. Comparing the grid pictures and the Mach contour plots one can clearly see the correlation between good grid resolution and flow structure sharpness. The classical composite meshing techniques, Figures 9a and 9b, waste mesh points in excessive refinement where, through the topology, zones of boundary layer mesh propagate out into the computational domain. The multiple independent patched mesh strategy, with single mesh cell overlap to exchange data by interpolation[42], permits better balanced resolution and use of mesh resources. The latter has small wraparound patches communicating the boundary layers around the sharp corners at the base.

Finally, Figures 11a and 11b show comparisons of computed base pressure against the experimental pressure tap data. Figure 11a shows that the double wraparound grid provides a good average base pressure prediction, but a wave structure due to cooperative vortex jet action in the separated flow region is an artifact of the calculation. The overall solution is substantially improved *vis a vis* earlier attempts by other workers with central difference methods and Cartesian step grids, Figure 12 from reference 15. Our results with Cartesian step grid is also somewhat less satisfactory than with the double wraparound grid.

Figure 11b shows that the independent multiple grid solution without adaptation performs qualitatively similar to the double wraparound grid in terms of the vortex action. However, the same topology with flow structure adaptive grid point redistribution provides the additional refinement and, likely also, alignment features to permit a subtle circulation mechanism to be set up in the modified base separation vortex pattern; and a correct flat pressure distribution results. Thus here the flow physics and associated qualitative solution structure are found to be

strongly influenced by grid topology and resolution. More details are available in references 30 and 32.

3. Publications

Two meeting papers in the area of algebraic grid generation have resulted, reference 33 and the paper in preparation: Luh, R.C.-C. and Lombard, C.K.: "FASTWO - A 2-D Interactive Algebraic Grid Generator," AIAA-88-0516.

Two meeting papers in the area of SOCBT flow analyses with the 2-D and 3-D CSCM-S codes have resulted, reference 29 and the paper in preparation: Bardina, Jorge, Lombard, C.K. and Luh, R.C.-C.: "CSCM Three Dimensional Navier-Stokes Computational Aerodynamics for a Projectile Configuration at Transonic Velocities", abstract submitted for AIAA 6th Applied Aerodynamics Conference, June 1988.

Three meeting papers, references 30-32, have resulted from the computational research in the MICOM propulsion base flow problem.

4. Scientific Personnel

Dr. C.K. Lombard, Principal Investigator
Dr. Jorge Bardina
Dr. Raymond C.-C. Luh
Dr. Ethiraj Venkatapathy

5. Bibliography

1. Beam, R.M. and Warming, R.F.: "An Implicit Factored Scheme for the Compressible Navier-Stokes Equations," AIAA-73-257, 1973.
2. Schiff, L.B. and Steger, J.L.: "Numerical Simulation of Steady Supersonic Viscous Flow," AIAA-79-0130, 1979.
3. Schiff, L.B. and Sturek, W.B.: "Numerical Simulation of Steady Supersonic Flow Over an Ogive-Cylinder-Boattail Body," AIAA-80-0066, 1980.
4. Sturek, W.B. and Schiff, L.B.: "Computation of the Magnus Effect for Slender Bodies in Supersonic Flow," AIAA-80-1586-CP, 1980.
5. Nietubicz, C.J.: "Navier-Stokes Computation for Conventional and Hollow Projectile Shapes at Transonic Velocities," AIAA-81-1262, 1981.
6. Nietubicz, C.J., Inger, G.R. and Danberg, J.E.: "A Theoretical and Experimental Investigation of a Transonic Projectile Flow Field," AIAA-82-0101, 1982.
7. Nietubicz, C.J., Sturek, W.B. and Heavey, K.R.: "Computation of Projectile Magnus Effect at Transonic Velocities," AIAA-83-0237, 1983.
8. Sahu, J., Nietubicz, C.J. and Steger, J.L.: "Navier-Stokes Computations of Projectile Base Flow with and without Base Injection," AIAA-83-0224, 1983.
9. Deiwert, G.S.: "Numerical Simulation of Three-Dimensional Boattail Afterbody Flow Field," AIAA-80-1347, 1980.
10. Deiwert, G.S.: "A Computational Investigation of Supersonic Axisymmetric Flow Over Boattails Containing a Centered Propulsive Jet," AIAA-83-0462, 1983.
11. Wagner, B.: "Calculation of Turbulent Flow About Missile Afterbodies Containing an Exhaust Jet," AIAA-84-1659, 1984.
12. Sahu, J. and Nietubicz, C.J.: "Numerical Computation of Base Flow for a Missile in the Presence of a Centered Jet," AIAA-84-0527, 1984.
13. Sahu, J.: "Computations of Supersonic Flow Over a Missile Afterbody Containing an Exhaust Jet," AIAA-85-1815, 1985.
14. Thomas, P.D., Reklis, R.P., Roloff, R.R. and Conti, R.J.: "Numerical Simulation of Axisymmetric Base Flow on Tactical Missiles with Propulsive Jet," AIAA-84-1658, 1984.
15. Petrie, H.L. and Walker, B.J.: "Comparison of Experiment and Computation for a Missile Base Region Flowfield with a Centered Propulsive Jet," AIAA-85-1618, 1985.
16. Putnam, L.E. and Bissinger, N.C.: "Results of AGARD Assessment of Prediction Capabilities for Nozzle Afterbody Flows," AIAA-85-1464, 1985.
17. Kayser, L.D. and Whiton, F.: "Surface Pressure Measurements on a Boattailed Projectile Shape at Transonic Speeds, ARBRL-MR-03161, U.S. Army Ballistic

Research Laboratory/ARRADCOM, Aberdeen Proving Ground, MD 21005, 1982.

18. Sturek, W.B., private conversation, 1983.

19. Baldwin, B.S. and Lomax, H.: "Thin Layer Approximation and Algebraic Model for Separated Turbulent Flows," AIAA-78-257, 1978.

20. Lombard, C.K., Oliger, J. and Yang, J.Y.: "A Natural Conservative Flux Difference Splitting for the Hyperbolic Systems of Gasdynamics," AIAA-82-0976, 1982.

21. Lombard, C.K., Oliger, J., Yang, J.Y. and Davy, W.C.: "Conservative Supra-Characteristics Method for Splitting the Hyperbolic Systems of Gasdynamics with Computed Boundaries for Real and Perfect Gases," AIAA-82-0837, 1982.

22. Lombard, C.K., Oliger, J. and Yang, J.Y.: "A Natural Conservative Flux Difference Splitting for the Hyperbolic Systems of Gasdynamics," *Proceedings of the 8th International Conference on Numerical Methods in Fluid Dynamics, Springer Lecture Notes in Physics 141*, 1982.

23. Lombard, C.K., Bardina, J., Venkatapathy, E. and Oliger, J.: "Multi-Dimensional Formulation of CSCM - An Upwind Flux Difference Eigenvector Split Method for the Compressible Navier-Stokes Equations," AIAA-83-1895, 1983.

24. Lombard, C.K., Venkatapathy, Ethiraj and Bardina, J.: "Universal Single Level Implicit Algorithm for Gasdynamics," AIAA-84-1533, 1984.

25. Lombard, C.K., Bardina, J. and Venkatapathy, E.: "AOTV Bluff Body Flow - Relaxation Algorithm," *Thermal Design of Aeroassisted Orbital Transfer Vehicles*, H.F. Nelson, Ed., *Progress in Astronautics and Aeronautics*, Vol. 96, 1985, pp 85-112.

26. Vinokur, M. and Lombard, C.K.: "Algebraic Grid Generation with Corner Singularities," *Advances in Grid Generation*, Vol. 5, Sponsored by ASME Fluids Engineering Div., Symposium on Grid Generation, 1983, ASME Fluids Engineering Conference, Houston, Texas.

27. Eiseman, P.R. and Smith, R.E.: "Mesh Generation Using Algebraic Techniques," *Numerical Grid Generation Techniques*, NASA CP 2166, 1980.

28. Thompson, J.F.: "A Survey of Grid Generation Techniques in Computational Fluid Dynamics," AIAA-83-0447, 1983.

29. Luh, Raymond Ching-Chung and Lombard, C.K.: "Projectile Aerodynamics Prediction with CSCM-S Upwind Implicit Relaxation Algorithm," AIAA-85-1838-CP, 1985.

30. Lombard, C.K., Luh, R. C.-C., Nagaraj, N., Bardina, J. and Venkatapathy, E.: "Numerical Simulation of Backward Step and Jet Exhaust Flows," AIAA-86-0432, 1986.

31. Lombard, C.K., Bardina, J., Venkatapathy, E., Yang, J.Y., Luh, R.C.-C., Nagaraj, N. and Raiszadeh, F.: "Accurate, Efficient and Productive Methodology for Solving Turbulent Viscous Flows in Complex Geometry," *Proceedings of the 10th International Conference on Numerical Methods in Fluid Dynamics, Springer Lecture Notes in Physics, 264*, 1986.

32. Venkatapathy, Ethiraj and Lombard, C.K.: "Accurate Numerical Simulation of Supersonic Jet Exhaust Flow with CSCM for Adaptive Overlapping Grids," AIAA-87-0436, 1987.

33. Luh, R. C.-C., Nagaraj, N. and Lombard, C.K.: "Simplified Algebraic Grid Generation in Patched Mesh Systems," AIAA-87-0200, 1987.

34. Luh, R. C.-C. and Lombard, C.K.: "FASTWO - A 2-D Interactive Algebraic Grid Generator," AIAA-88-0516, 1988.

35. Bardina, J. and Lombard, C.K.: "Three Dimensional Hypersonic Flow Simulations with the CSCM Implicit Upwind Navier-Stokes Method," AIAA-87-1114-CP, 1987.

36. Bardina, J., Lombard, C.K. and Luh, R. C.-C.: "CSCM Three Dimensional Navier-Stokes Computational Aerodynamics for a Projectile Configuration at Transonic Velocities," Abstract presented for the AIAA 6th Applied Aerodynamics Conference, June 1988.

37. Vinokur, M.: "On One-Dimensional Stretching Functions for Finite-Difference Calculations," *J. Comp. Physics*, Vol. 50, No. 2, May 1983.

38. Yang, J.Y., Lombard, C.K. and Bardina, Jorge: "Implicit Upwind TVD Schemes for the Euler Equations with Bidiagonal Approximate Factorization," Presented at the *International Symposium on Computational Fluid Dynamics-Tokyo*, 1985.

39. Venkatapathy, E., Lombard, C.K. and Nagaraj, N.: "Numerical Simulation of Compressible Flow Around Complex Two-Dimensional Cavities," AIAA-87-0116, 1987.

40. Bardina, J., Venkatapathy, E. and Lombard, C.K.: "CSCM Methodology for Cavity Flow Design in a Supersonic Wedge Flow," AIAA-87-0518, 1987.

41. Venkatapathy, E., Nystrom, G.A., Bardina, J. and Lombard, C.K.: "Application of the CSCM Method to the Design of Wedge Cavities," AIAA-87-1317, 1987.

42. Lombard, C.K. and Venkatapathy, Ethiraj: "Implicit Boundary Treatment for Joined and Disjoint Patched Mesh Systems," AIAA-85-1503, 1985.

43. Vigneron, Y.C., Rakich, J.V. and Tannehill, J.C.: "Calculation of Supersonic Viscous Flow over Delta Wings with Sharp Subsonic Leading Edges," NASA TM-78500, 1978.

44. Rai, M.M., Chaussee, D.S. and Rizk, Y.M.: "Calculation of Viscous Supersonic Flows Over Finned Bodies," AIAA-83-1667, 1983.

45. Bardina, J. and Lombard, C.K.: "Three Dimensional CSCM Method for the Compressible Navier-Stokes Equations with Application to a Multi-Nozzle Exhaust Flowfield," AIAA-85-1193, 1985.

46. Stookesberry, D.C.: "Computation of Separated Flow on a Ramp Using the Space Marching Conservative Supra-Characteristics Method," Master's Thesis, Dept. of Aerospace Engineering, Iowa State University, Ames, IA, 1985.

47. Codding, W.H., Lombard, C.K. and Yang. J.Y.: "CSCM Navier-Stokes Thermal/Aerodynamic Analysis of Hypersonic Nozzle Flows with Slot Injection and Wall Cooling," Abstract submitted for the AIAA 6th Applied Aerodynamics Conference, June 1988.

48. Roe, P.L.: "The Use of the Riemann Problem in Finite-Difference Schemes," *Proceedings of the Seventh International Conference on Numerical Methods in Fluid Dynamics, Springer Lecture Notes in Physics, 141*, pp 354-359, 1981.

49. Oliger, Joseph and Lombard, C.K.: "Boundary Approximations for Alternating Sweep Implicit Upwind Methods for Hyperbolic Systems," SIAM 1983 Fall Meeting, Norfolk, VA.

50. Steger, J.L.: "Implicit Finite Difference Simulation of Flow About Arbitrary Geometries with Application to Airfoils," AIAA-77-665, 1977.

51. Sahu, J.: "Three Dimensional Base Flow Calculation for a Projectile at Transonic Velocity," AIAA-86-1051, 1986.

52. Nietubicz, C.J., Mylin, D.C., Sahu, J. and Lafarge, R.: "Aerodynamic Coefficient Predictions for a Projectile Configuration at Transonic Speeds," AIAA-84-0326, 1984.

53. Nakahashi, K. and Deiwert, G.S.: "A Self-Adaptive-Grid Method with Application to Airfoil Flow," AIAA-85-1525, 1985.

Figure 1 SOCBT Grid Generation

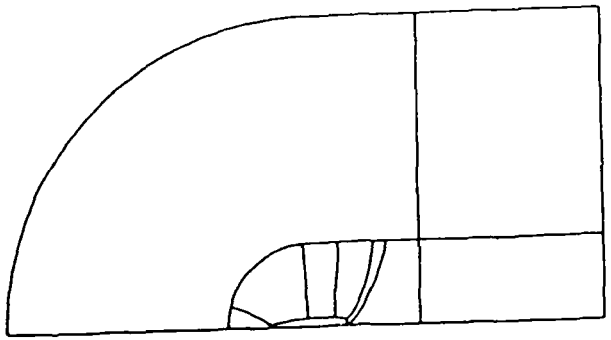

a. Patch Boundaries

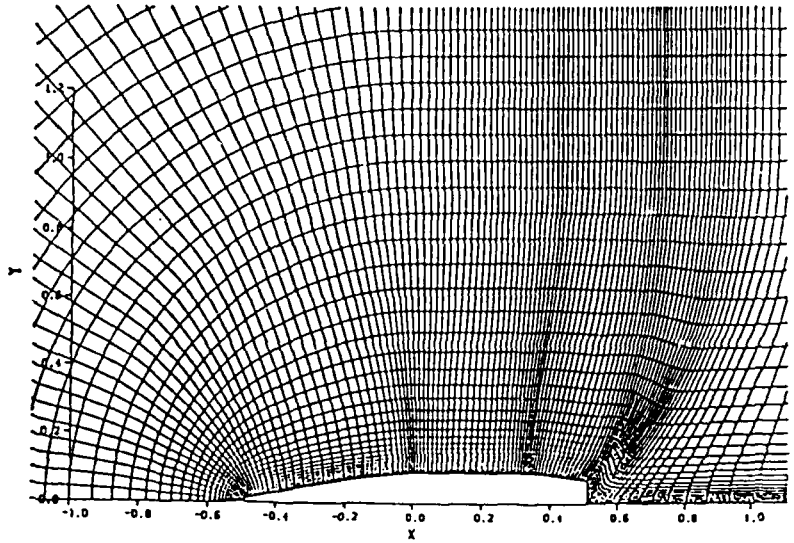

c. Near Field

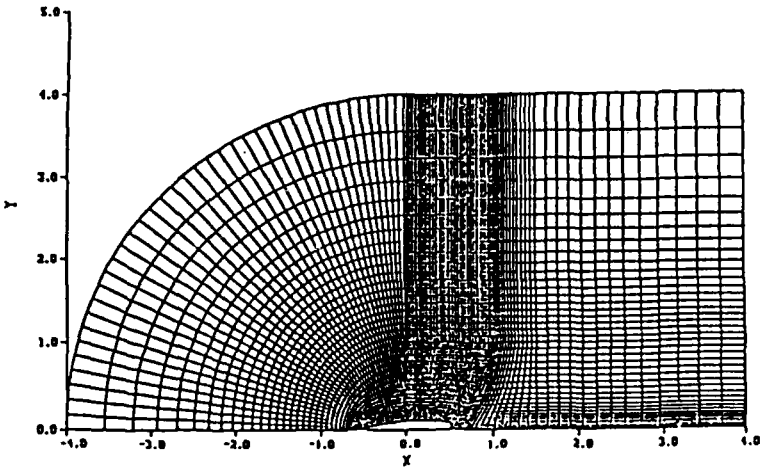

b. Complete Grid

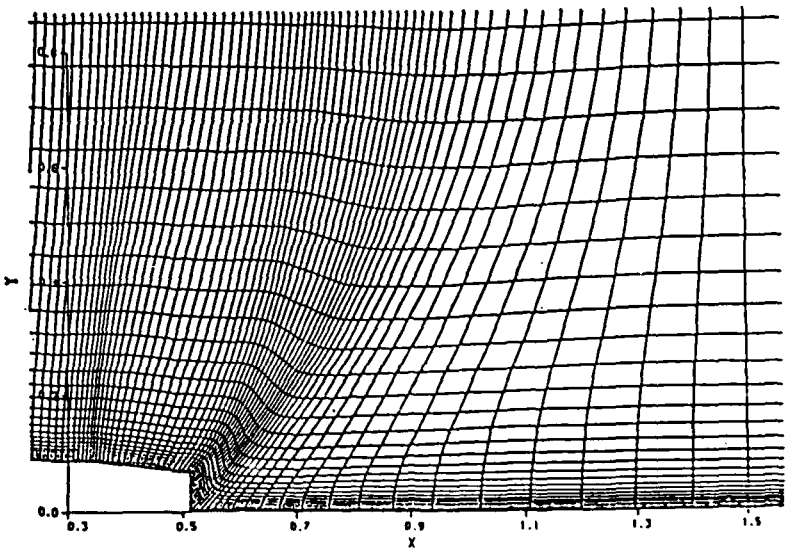

d. Base Region

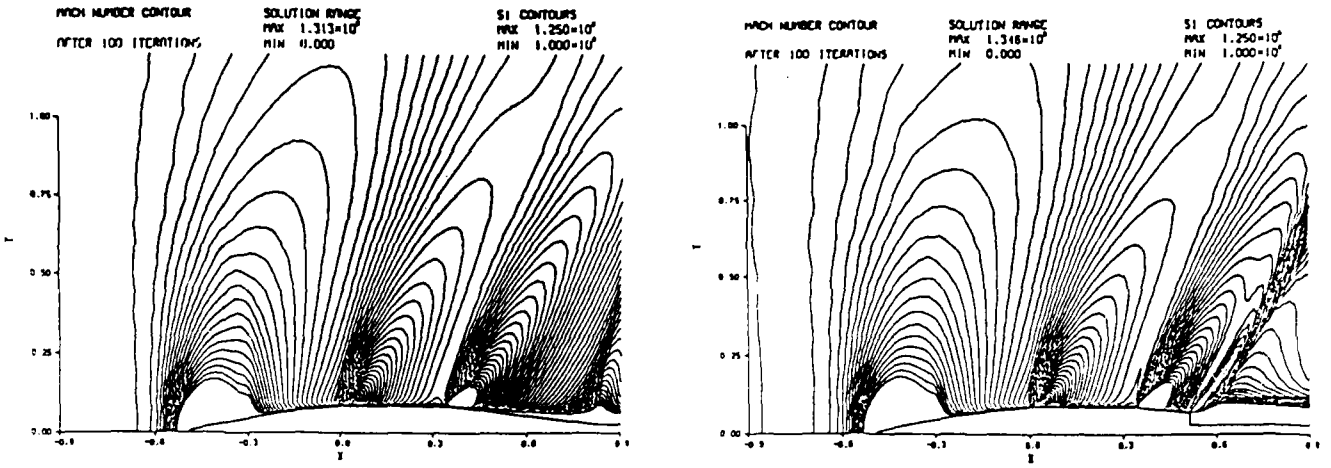

a. Boattail Continued Afterbody

b. Sting Mounted Base

Figure 2 Mach Contour Plots for SOCBT at Mach 1.1 Freestream

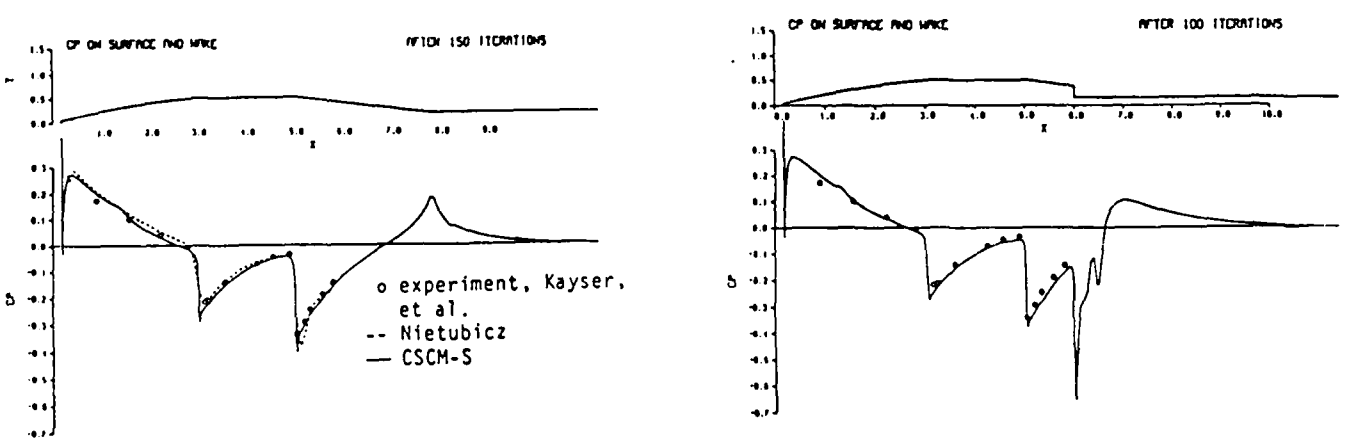

a. Boattail Continued Afterbody

b. Sting Mounted Base

Figure 3 C_p Plots for SOCBT at Mach 1.1

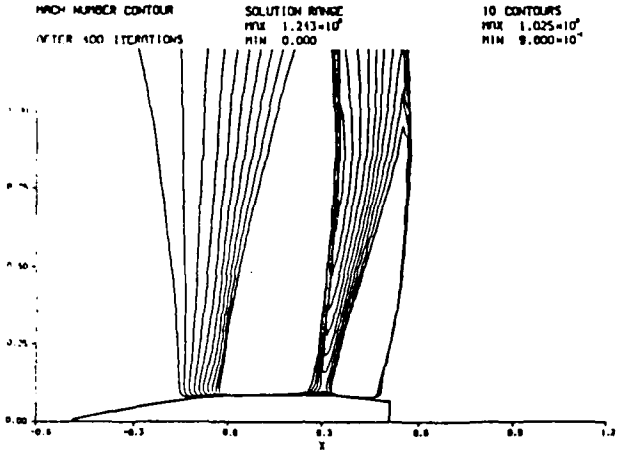

a. Mach Contours Free Flight Base

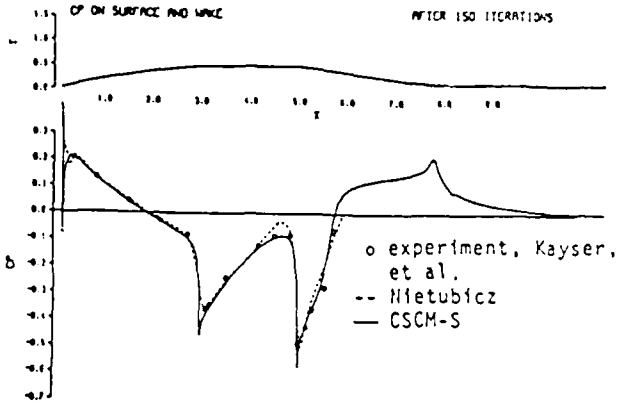

b. C_p, Boattail Continued Afterbody

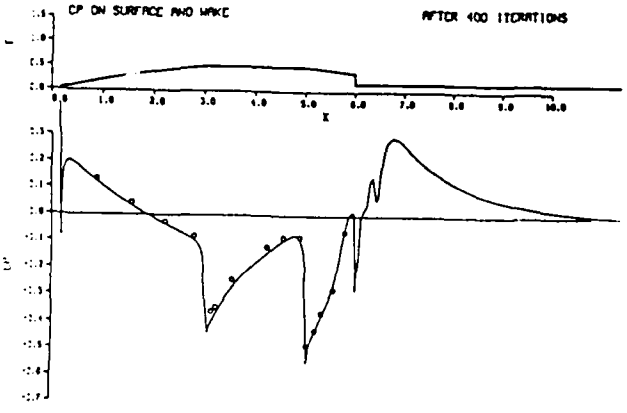

c. C_p, Sting Mounted Base

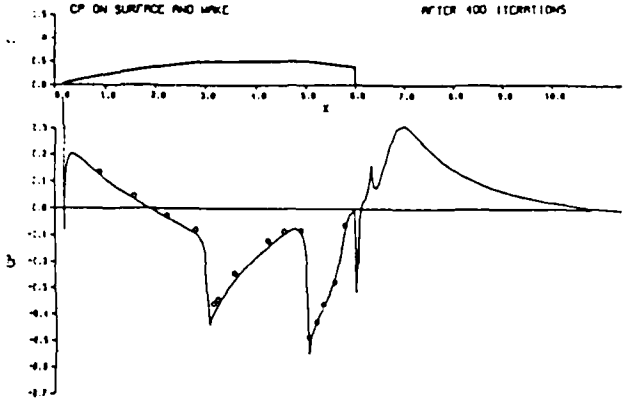

d. C_p, Free Flight Base

Figure 4 Plots for SOCBT at Mach 0.98

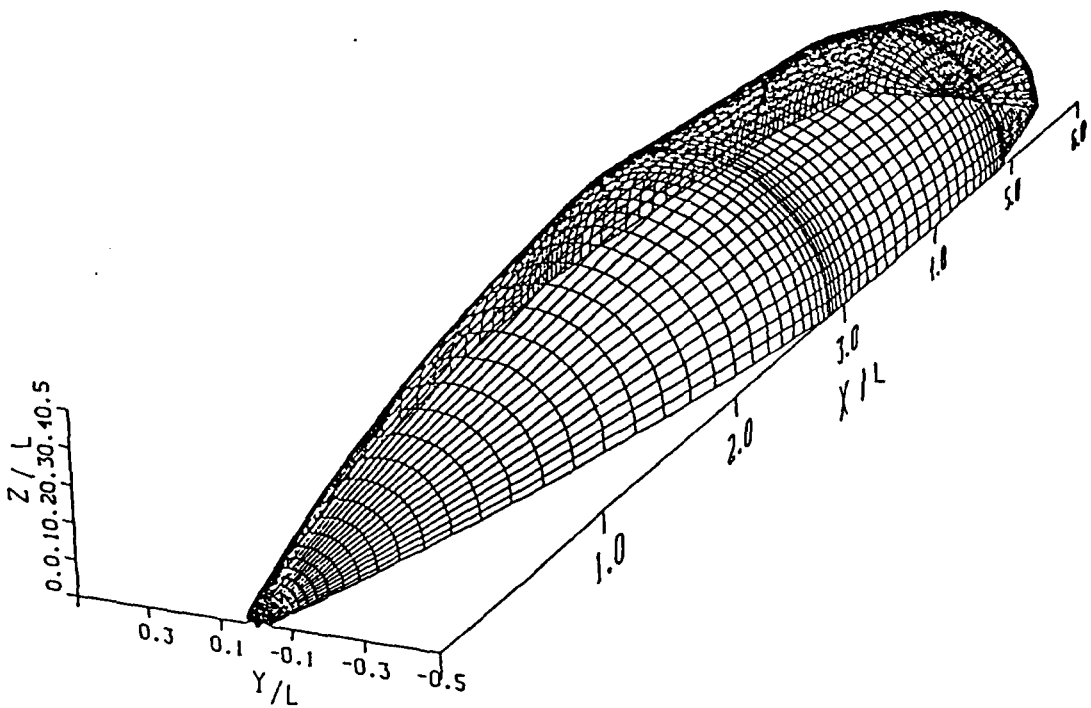

Figure 5 Perspective View of the SOCBT Surface Grid for the Symmetry Half Body

Figure 6 C_p Plots for SOCBT at Mach 0.96, Angle of Attack 4°

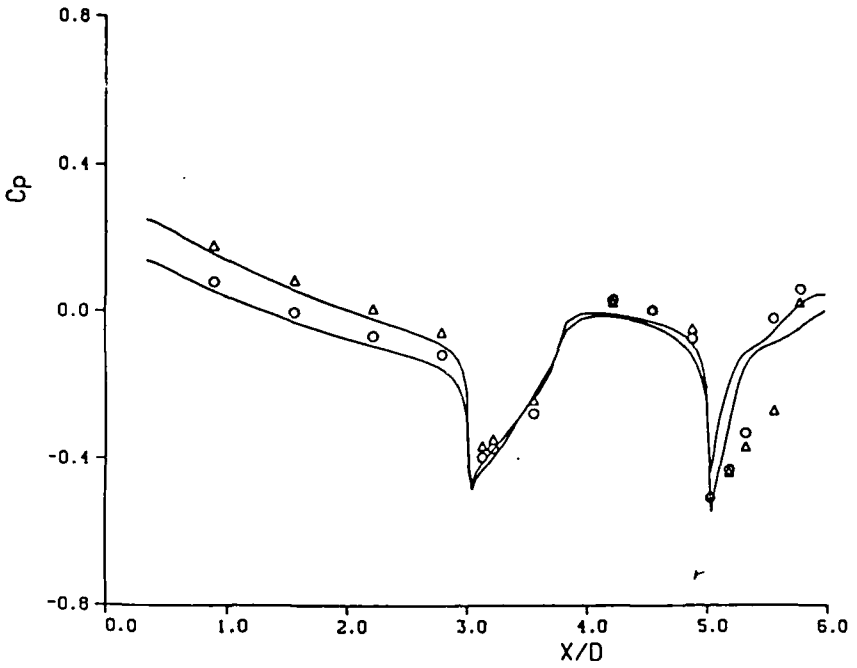

a. CSCM-S

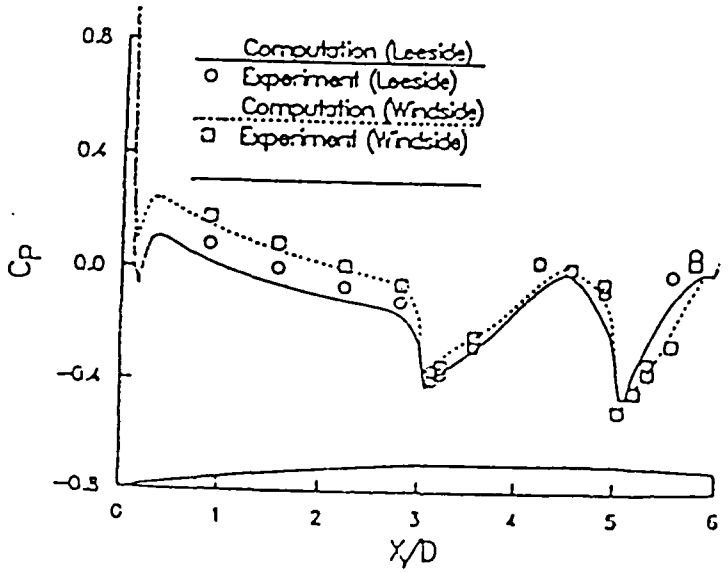

b. Sahu[51]

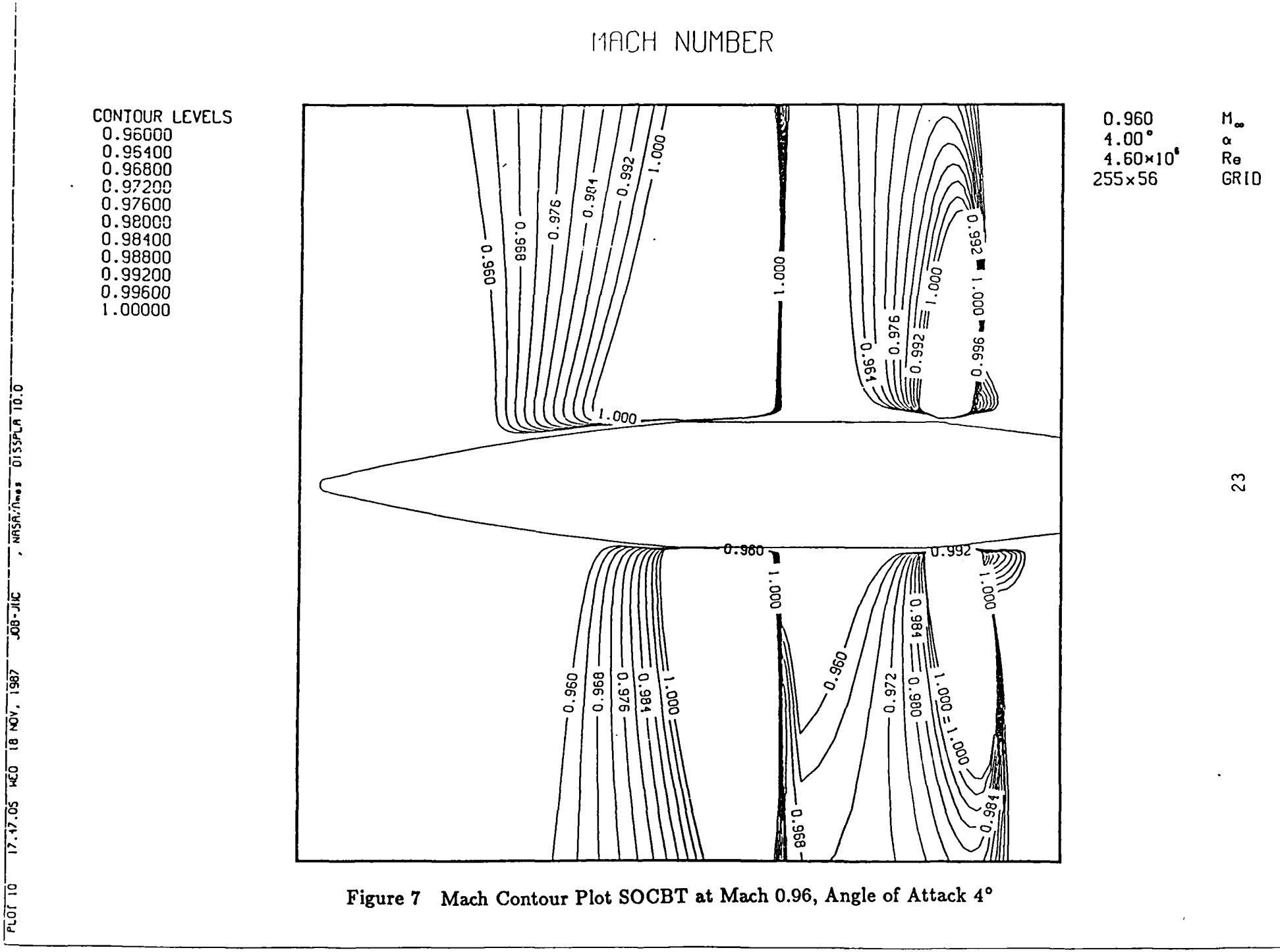

Figure 7 Mach Contour Plot SOCBT at Mach 0.96, Angle of Attack 4°

Figure 8 C_p Plots for SOCBT at Mach 0.95, Angle of Attack 2°

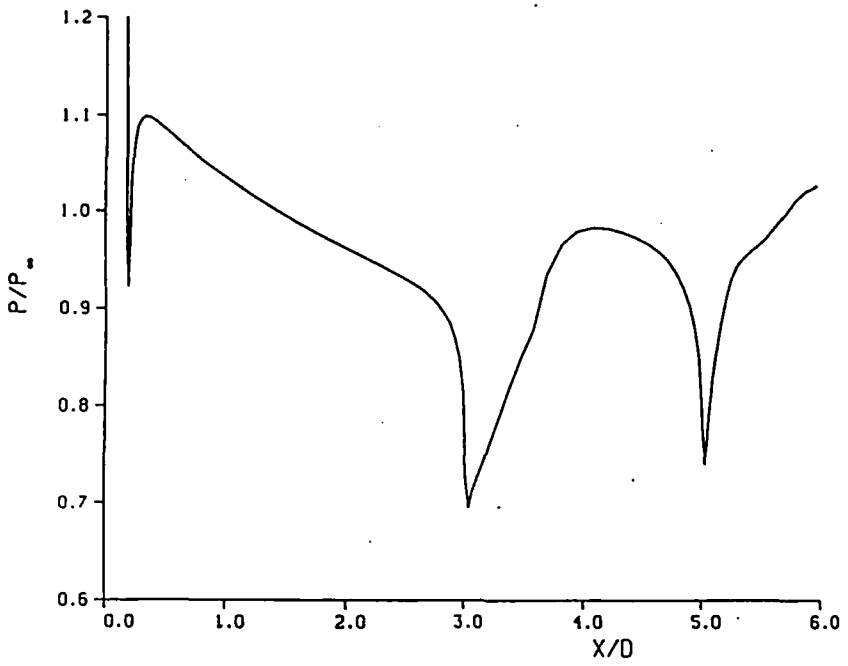

a. CSCM-S

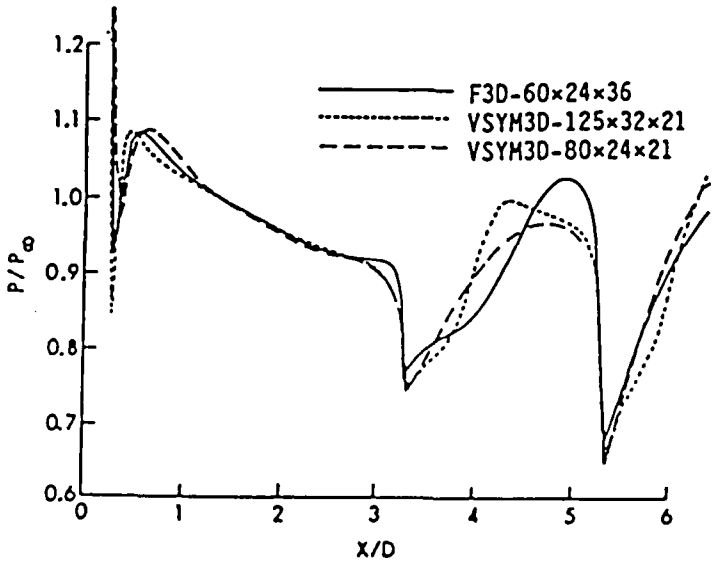

b. Nietubicz, et al[52]

Figure 9 Grids for MICOM Base Flow Study

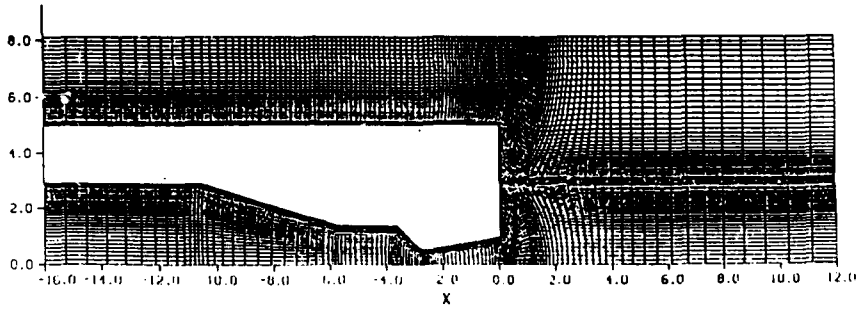

a. Composite, Double Wraparound

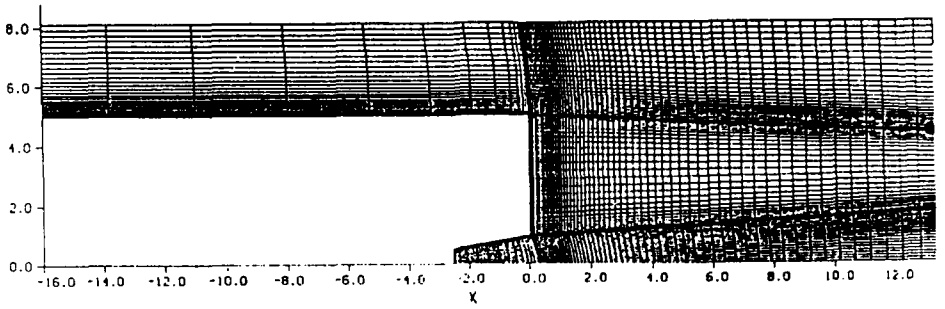

b. Composite, Cartesian Step

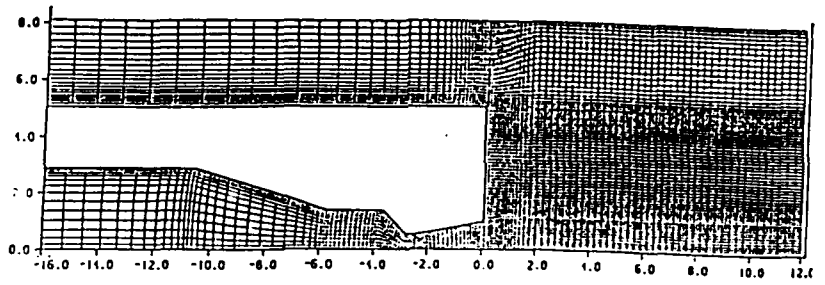

c. Overset, Multiple Patch

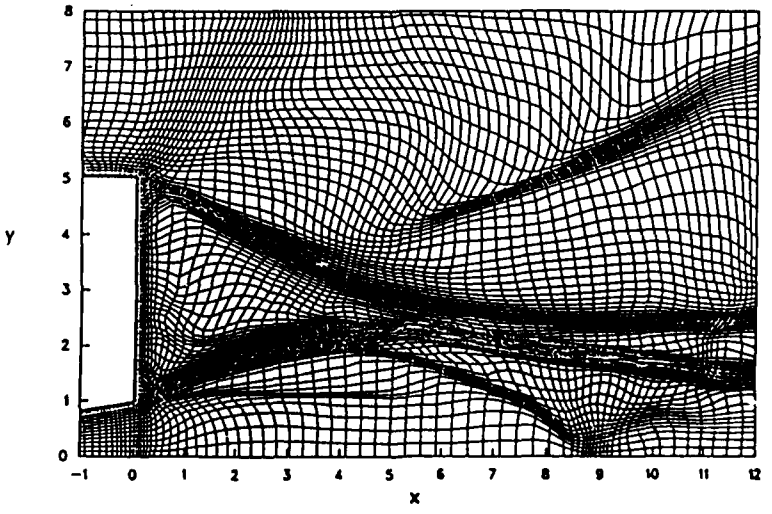

d. Solution Adaptive from (c)

Figure 10 Mach Contour Plots for MICOM Base Flow Computed with CSCM-S

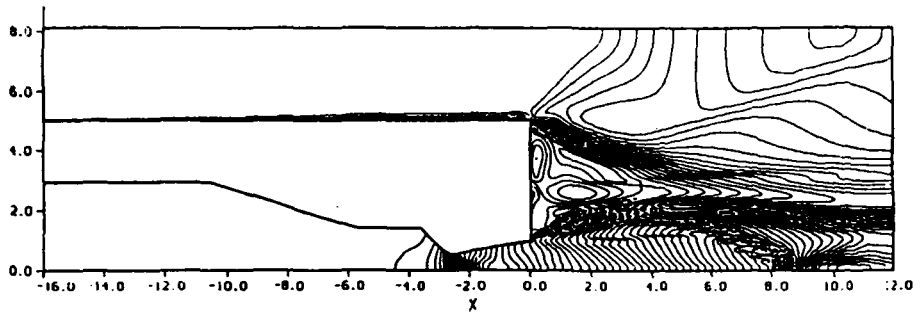

a. Composite, Double Wraparound

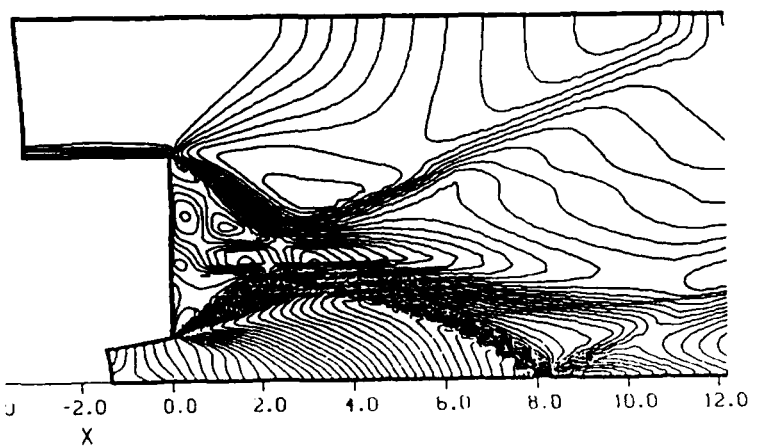

b. Composite, Cartesian Step

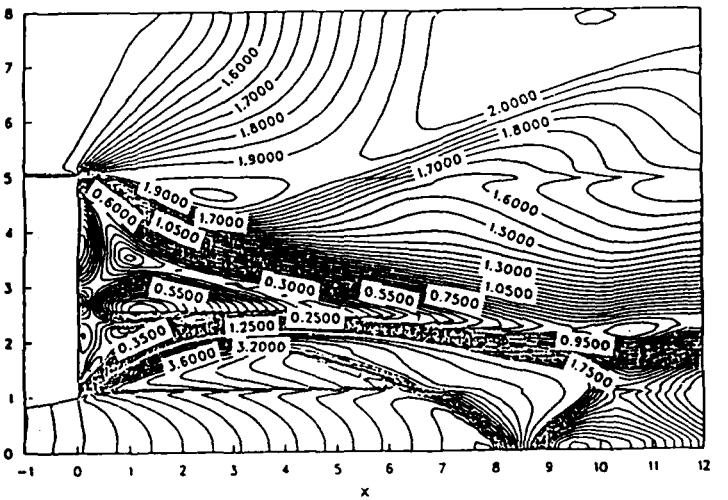

c. Overset, Multiple Patch

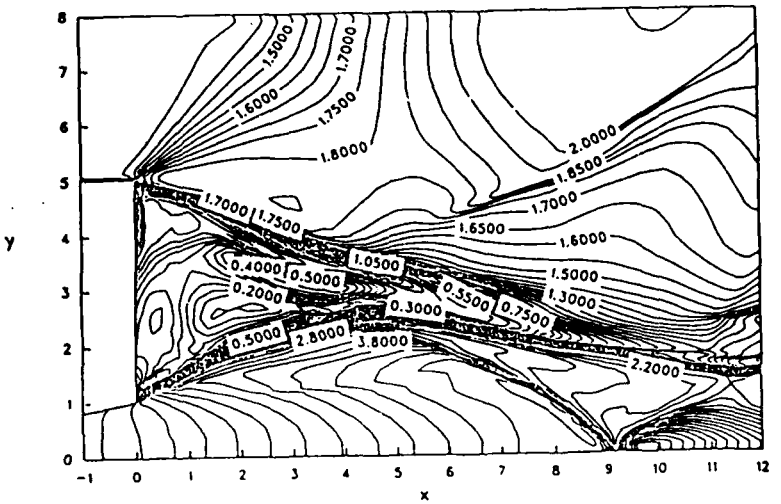

d. Solution Adaptive from (c)

Figure 11 Base Pressure Plots for MICOM Base Flow Computed with CSCM-S

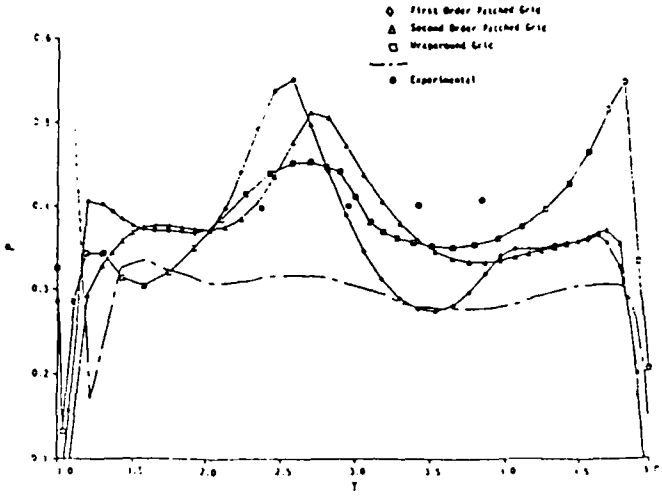

a. Composite Grid Results

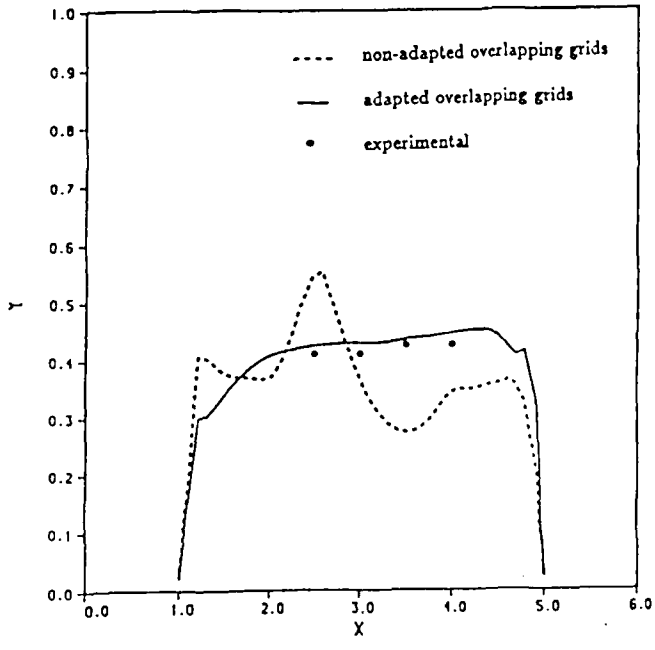

b. Overset Grid Results

BASE PRESSURE COMPARISONS

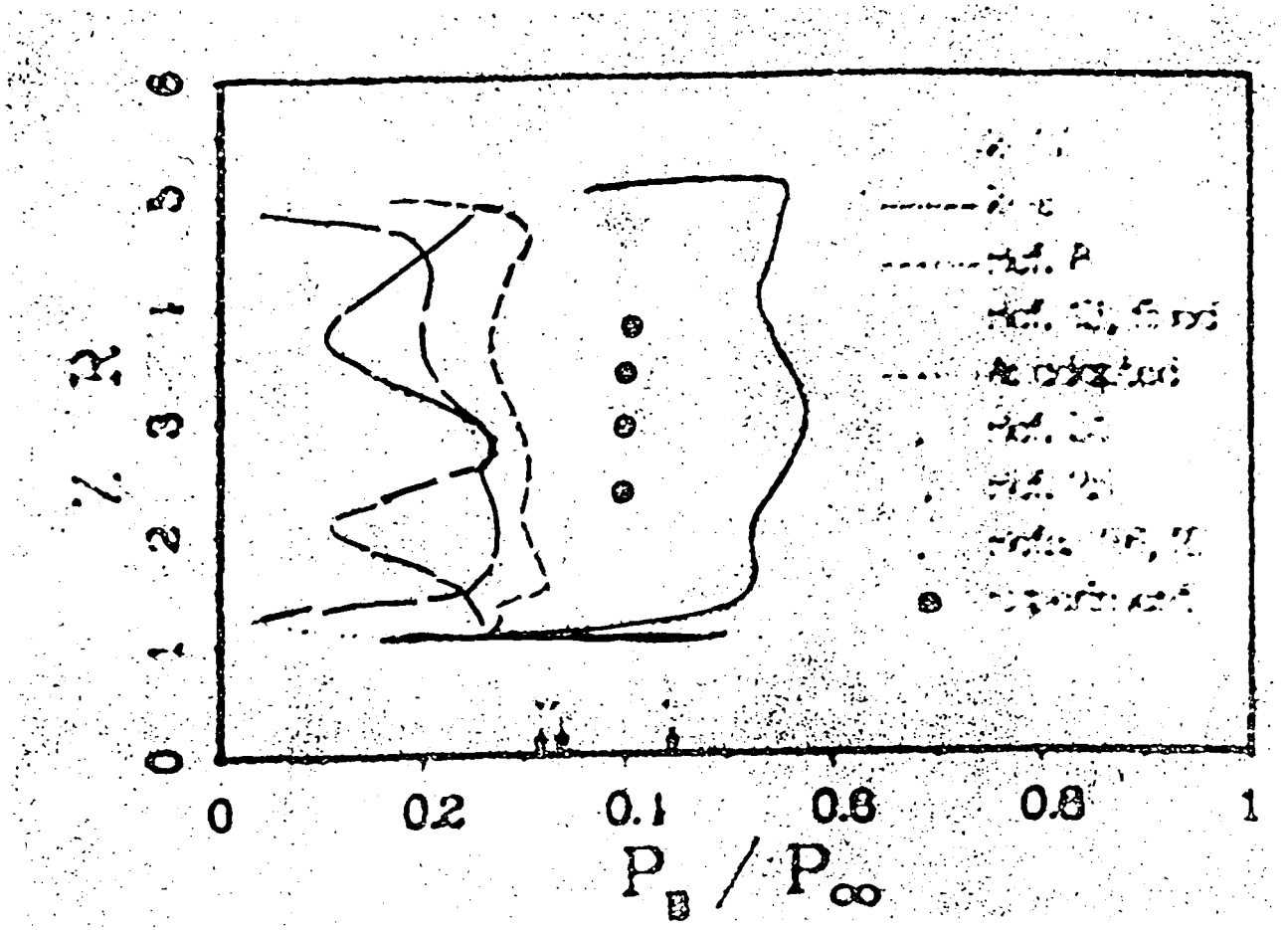

Figure 12 Base Pressure Plots for MICOM Base Flow from Earlier Studies[15] with Other Methods

END

DATE

FILMED

5-88

DTIC